Proceedings of the
Third International Symposium on Scale Modeling
September 10-13, 2000, Nagoya, Japan

ISSM3-C8

MARGINALLY FLAMMABLE MATERIALS: BURNING VELOCITY OF TRANS-DICHLOROETHYLENE

G.T. LINTERIS, and V. I. BABUSHOK

Fire Science Division; Building and Fire Research Laboratory
National Institute of Standards and Technology
Gaithersburg, MD 20899-8651

Key Words: chlorinated hydrocarbons, dichloroethylene, flame speed,

ABSTRACT

The overpressure dynamics and explosion hazard of commodity materials under full-scale conditions are often assessed through laboratory measurements of their laminar burning velocity. We present the first measurements of the flame speed of trans-1,2-dicholorethylene (TDCE). Data are presented for a fuel stream consisting of TDCE/methane blends (in which the TDCE mole fraction is up to 0.9) for combustion with air at a fuel-air equivalence ratio ϕ of 1.0, 1.1 and 1.2. Data are also presented for stoichiometric flames of pure TDCE with the oxidizer stream having a range of oxygen mole fraction from 0.27 to 0.365, and at two values of the oxidizer oxygen mole fraction (0.32 and 0.365) over a range of equivalence ratio ($0.65 <= \phi <= 1.2$). Extrapolations of the results with TDCE/methane blends and with higher oxygen mole fraction to the conditions of flames of pure TDCE with air at ϕ=1.0 indicate a laminar burning velocity of (10.7±1.2) cm/s. In general, the results indicate that the TDCE burning velocity is about one fourth that of methane. For TDCE, the maximum burning velocity occurs for slightly fuel lean conditions. Numerical modeling of the burning velocity yields values about a factor of two lower than the experiments, suggesting that improvements in the kinetic description are required.

INTRODUCTION

Many marginally flammable materials are used or produced to meet residential, commercial, or industrial needs. In order to understand the explosion and detonation hazards of these compounds, it is necessary to scale their combustion properties, determined from laboratory tests, to full-scale conditions relevant to their use. One of the most widely used parameters for such scaling (Zalosh, 1995) is the laminar burning velocity S_L, which is a fundamental physico-chemical parameter describing the rate of propagation of a flame into a quiescent mixture of the compound with air. The determination of the burning velocity for these compounds is challenging, however, because the magnitude is low. As an example, the present paper discusses measurements of the burning velocity of one such compound, dichloroethylene.

Trans-1,2-dichloroethylene $C_2H_2Cl_2$ (TDCE) is a low-temperature extraction solvent for organic materials, and is an intermediate in the synthesis of other chlorinated ethylenes (Mertens, 1991). Recently, it has been used in blends with chlorofluorocarbons (CFCs) for vapor-phase solvent cleaning, replacing other CFCs which have undesirable ozone depletion potentials. It has a boiling point of 47.7 °C, a flash point of 4 °C, and explosion limits of 5.6 % to 12.8 % mole fraction in air. Because of these characteristics, the possibility exists for its

accidental ignition and combustion. Measured values of its burning velocity will be of use for predicting the overpressure potential and the venting requirements following its ignition.

It is also of interest to study the combustion of TDCE because of its relevance to toxic waste incineration. TDCE will be formed as an intermediate species in the combustion of other chlorinated hydrocarbons CHCs, including chloromethanes (Qun and Senkan, 1994). Flame structure measurements for blends of TDCE/CH_4 have been reported (Castaldi and Senkan, 1996) for TDCE/CH_4 ratios of 0.27 to 0.40; however, no data exist for combustion of the pure compound. Measured burning velocities for pure TDCE can provide data for development and testing of comprehensive chemical kinetic mechanisms of CHC combustion outside of the range of conditions for which the models have been assembled, extending their range of applicability. Kinetic mechanisms, validated over a range of relevant conditions, are of use for scale modeling, either through their direct application, or through their use in developing reduced kinetic mechanisms.

EXPERIMENT

A Bunsen-type nozzle burner based on the design of Mache and Hebra (1941) is used to obtain the laminar burning velocities. The experimental system has been described in detail previously (Linteris and Truett, 1996; Linteris et al., 2000). The burner consists of a quartz tube 27 cm long with an area contraction ratio of 4.7 (over a 3 cm length) and a final nozzle diameter of (1.02 ± 0.005) cm, which is placed in a square acrylic chimney 10 cm wide and 86 cm tall, with provision for co-flowing air or nitrogen gas. An optical system (a white-light source with a vertical slit at its exit, lenses, a vertical band, and filters) (Van Wonterghem and Van Tiggelen, 1954) generates the schlieren image of the flame for capture by a 776 x 512 pixel Charged Injection Device (CID) array (Cidtec CID3710D)[1]. The image is digitized by a 640 x 480 pixel frame-grabber board (Data Translation 3155) in a Pentium-II computer. The images are acquired and written to disk using the free University of Texas Health Science Center of San Antonio ImageTool program (UTHSCA, 1996). The burner produces straight-sided schlieren and visible images which are very closely parallel. The flame area is determined (assuming axial symmetry) using custom image-processing software, and the burning velocity is calculated by dividing the volumetric flow rate (corrected to 101 kPa and 298 K) by the flame area (Andrews and Bradley, 1972).

[1] Certain commercial equipment, instruments, or materials are identified in this paper to adequately specify the procedure. Such identification does not imply recommendation or endorsement by the National Institute of Standards and Technology, nor does it imply that the materials or equipment are necessarily the best available for the intended use.

Gas flows are measured with digitally-controlled mass flow controllers (Sierra Model 860) with a quoted repeatability (by the manufacturer) of 0.2 % and accuracy of 1 % of full-scale flow which have been calibrated with piston (Bios Intl. DCL-20K) and dry (American Meter Co. DTM-200A) flow meters so that the expanded uncertainty of the indicated flow is 1.5 %. House compressed air (filtered and dried) is used after it has been additionally cleaned by passing it through an 0.01 μm filter, a carbon filter, and a desiccant bed to remove small aerosols, organic vapors, and water vapor. The fuel is trans-1,2-dicholorethane, alone or with methane (Matheson UHP, 99.9 %); and the oxidizer stream consists of laboratory air, or a blend of nitrogen from liquid N_2 boil-off, and oxygen (MG Industries, H_2O < 50 ppm; total hydrocarbons < 5 ppm). The laboratory air has a relative humidity of about 5 %, while the synthetic air has less than 10 ppm of H_2O.

For addition of the liquid fuel, two computer-controlled stepper-motor driven syringe pumps (Yale Apparatus model YA-12) located in a chemical fume hood feed the fuel at room temperature (21.5 °C) through a series of check valves. The system allows accurate delivery of small volumes of liquid nearly continuously (one pump feeds fluid while the other withdraws fluid from the supply reservoir, and there is a slight discontinuity in the flow rate when the syringe pumps change direction). The liquid flows to an evaporator which consists of a stainless steel tube, 2.36 cm I.D. and 30.5 cm long, packed with 3mm diameter glass beads. Resistive heating wires and insulation surround the tube, and a single temperature controller maintains the temperature at the point of liquid injection to 60 °C . Fuel enters through a 3.2 mm O.D. stainless steel tube, and the oxidizer gas carries the liquid through the packed bed where it evaporates. The peak temperature downstream of the fuel injection reaches 150 °C during some tests. Precision glass/Teflon syringes (Hamilton Gas-tight, 2.5, 5.0, 10, 25, and 50 cc) provide gas-tight seals and relatively smooth operation of the liquid feed system. The smallest syringe possible is selected from the collection to provide the fastest piston speed with a long enough test time before syringe pump direction reversal (data collection is halted during syringe pump reversal). Prior to their entry into the burner, the reactant gases are cooled to room temperature by heat conduction from the transfer tubing.

For the present data, the visible flame height is maintained at constant value of 1.3 cm to provide similar rate of heat loss to the burner, while the desired equivalence ratio is preserved. The measured flame temperature is about 150 K less than the adiabatic flame temperature (Linteris and Truett, 1996), facilitating comparisons with the numerical calculations for a one-dimensional, freely propagating flame. Although the burning velocity in Bunsen-type flames is known to vary at the tip and base of the flame and is influenced by curvature and

stretch, these effects are most important over a small portion of the flame.

The uncertainty analysis consists of calculation of individual uncertainty components and root mean square summation of components. All uncertainties are reported as *expanded uncertainties*: $X \pm U$, where U is ku_c, and is determined from a combined standard uncertainty (estimated standard deviation) u_c, and a coverage factor $k = 2$ (level of confidence approximately 95%). Likewise, when reported, the relative uncertainty is $U / X \cdot 100\%$, or $ku_c / X \cdot 100\%$. Uncertainties in the equivalence ratio and oxygen mole fraction are 2.0 % and 1.4 % respectively. Uncertainties in the extrapolated values of the burning velocity represent the maximum relative uncertainty in the data used in the curve fit. No attempt is made to estimate the errors (unknown) in the extrapolation.

NUMERICAL

One-dimensional freely-propagating premixed flames are simulated using the Sandia flame code *Premix*, (Kee et al., 1991) the *Chemkin* subroutines (Kee et al., 1989), and the transport property subroutines (Kee et al., 1986). The initial temperature is 298 K and the pressure is 101.325 kPa.

The kinetic model used in this work is from Babushok and Tsang (2000). This mechanism is based mostly on models for the combustion of tetrachloromethane in methane/air mixtures (Leylegian et al., 1998) and for the high temperature oxidation of 1,1,1-trichloroethane (Thomson et al., 1994). The C_1-C_2 kinetic mechanism is from the work of Noto et al. (1998). A number of other reactions were added from the NIST Chemical Kinetics Data Base (Mallard et al., 1994) and other sources (Qun and Senkan, 1994; Thomson et al., 1994; Ho et al., 1995; Leylegian et al., 1998). The model used contains 632 reactions and 83 species. It includes reactions with:

H/Cl species (Cl, Cl_2 , HCl),
H/Cl/O species (ClO, HOCl),
$C/H_x/Cl_y$ species, (except the CCl radical),
C/H/Cl/O species (CH_2ClO, CHClO, $COCl_2$, COCl)
$C_2/H_x/Cl_y$ species, except C_2Cl radical.

Oxygenated C_2 chlorohydrocarbon species and their reactions are not considered.

The core of the kinetic model consists of the reactions for CCl_4 combustion in methane/air mixtures, and this sub-mechanism has been tested through comparisons of calculated and measured burning velocities for methane/air flames with added CH_3Cl, CH_2Cl_2, CH_3Cl and CCl_4 (Leylegian et al., 1998; Leylegian et al., 1998). Previous versions of this core sub-mechanism were also validated through the modeling of the combustion of hydrocarbons with added C_2Cl_4 (Wang et al., 1996; Wang et al., 1997) as well as through the modeling of chloromethane combustion in shock tube and flow reactor conditions. (Wang et al., 1996). In addition to these previous validations of the sub-mechanisms, limited testing of the kinetic mechanism of the present work was performed through comparisons of the measured and calculated ignition delays for chlorohydrocarbon addition behind shock waves (Wang et al., 1996).

RESULTS AND DISCUSSION

Flames of pure TDCE with air can be stabilized in the nozzle burner. Unfortunately, the flame shape was not amenable to accurate flame speed measurements: the flame was lifted, the flame position above the burner oscillated, and the schlieren image was not straight-sided, indicating a strong variation of the burning velocity over the flame surface. In order to determine the approximate burning velocity of pure flames of TDCE with air, we used two approaches. In the first, we combined TDCE with methane in varying proportions, and extrapolated to zero methane content. In the second, we performed experiments with pure TDCE at $\phi = 1.0$, but with oxygen mole fraction in the oxidizer stream $X_{O_2,ox}$ varying from 0.27 to 0.365 so that stable flames could be formed. The results are then extrapolated back to $X_{O_2,ox} = 0.21$. Finally, we also conducted experiments with pure TDCE at $X_{O_2,ox} = 0.32$ and 0.365 over a range of stoichiometry to provide new data for testing kinetic mechanism of TDCE reaction.

Figure 1 shows the measured burning velocity of mixtures of TDCE and methane as a function of the fraction of TDCE in the fuel stream $X_{TDCE}/(X_{TDCE}+X_{CH_4})$. A value of 0 corresponds to pure methane, and a value of 1 corresponds to pure TDCE. The figure shows the flame speed for three values of the fuel – air equivalence ratio ϕ (1.0, 1.1, and 1.2). The results of the numerical calculations are shown by the dotted line for ϕ=1.0. Note that the stoichiometric air requirement for TDCE and methane is the same, and the stoichiometry is calculated assuming reaction to the most stable products: H_2O, CO_2, CO, and HCl. Flames with ϕ =1.0 and 1.1 could be stabilized up to $X_{TDCE} = 0.8$ ($X_{CH_4} = 0.2$), and those with ϕ=1.2, up to $X_{TDCE} = 0.9$ ($X_{CH_4} = 0.1$). For the conditions of the tests, replacing the methane with TDCE reduces the burning velocity approximately linearly.

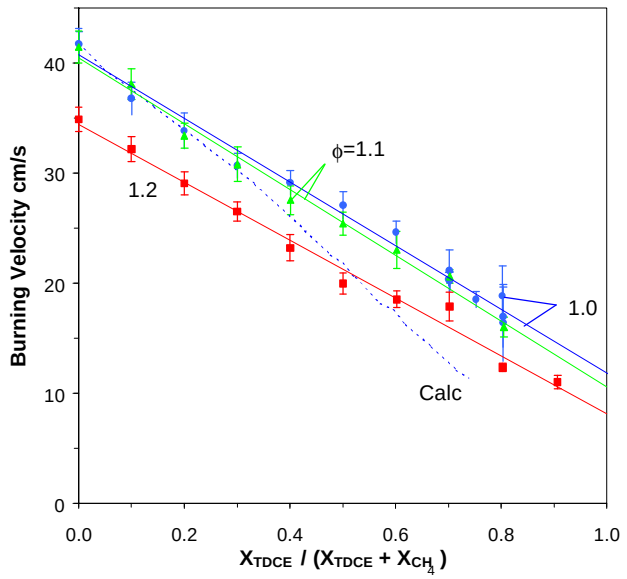

Figure 1 – Burning velocity of TDCE – methane mixtures for ϕ =1.0, 1.1, and 1.2 as a function of the molar fraction of TDCE in the fuel stream.

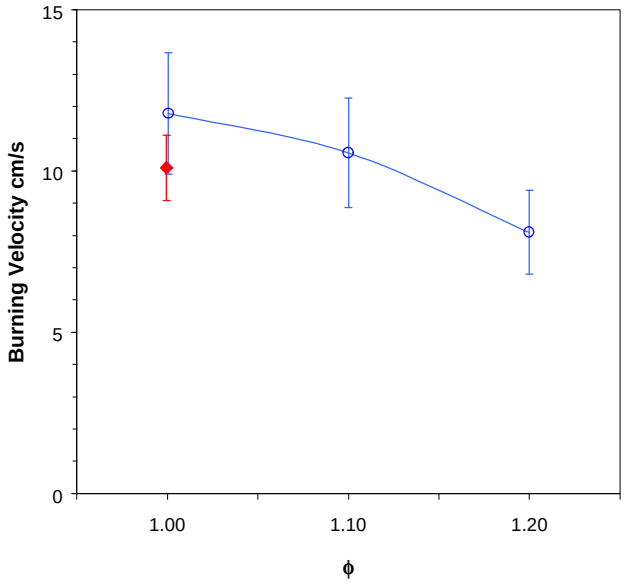

Figure 2 – Burning velocity of pure TDCE as a function of ϕ, from the extrapolation of methane/TDCE mixtures to pure TDCE (circles) and of varying $X_{O_2,ox}$ to $X_{O_2,ox}$=0.21 at ϕ=1.0 (diamond).

The values of the burning velocity extrapolated to conditions of pure TDCE are (11.8±1.9), (10.5±1.7), and (8.3±1.3) cm/s for ϕ=1.0, 1.1, and 1.2 respectively, as shown in Figure 2. Although we could not stabilize lean flames of TDCE with our burner, it appears from Figure 2 that the maximum flame speed would occur for lean flames (ϕ < 1.0). The pure TDCE flames appear to have a burning velocity about ¼ that of pure methane.

Figure 3 presents the experimental data (points) of tests with pure TDCE at ϕ=1.0 using synthetic air with increased oxygen content. For flames with increased $X_{O_2,ox}$, the burning velocity increases. A linear curve fit (solid line) indicates that extrapolating to a value of $X_{O_2,ox}$ = 0.21 yields a value of the burning velocity equal to (10.1±1.0) cm/s. This value is also presented on Figure 2, and shows reasonable agreement with the extrapolation of the results from the TDCE/methane blends. In Figure 3, the calculated burning velocity is shown by the dotted line.

Experiments with O_2-enriched air ($X_{O_2,ox}$ = 0.32 and 0.365) were also conducted for variable values of ϕ. The measured burning velocity of pure TDCE flames as a function of ϕ is shown in Figure 4 by the points. The solid lines show curve fits to the experimental data and the dotted line shows the prediction of the numerical calculation.

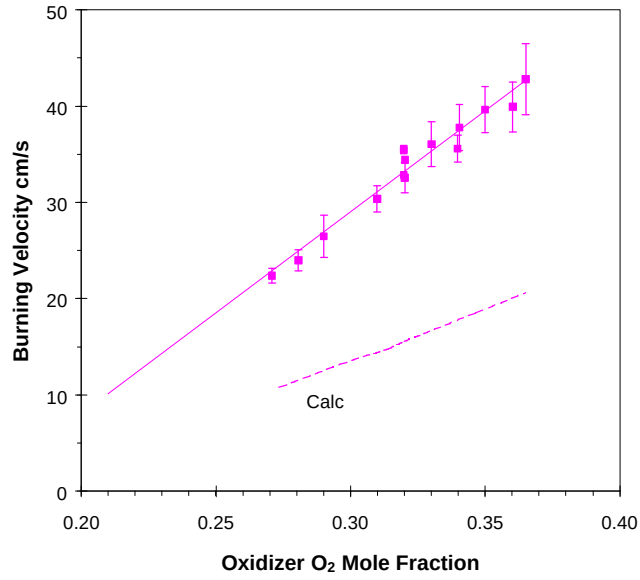

Figure 3 – Burning velocity of pure TDCE/O_2/N_2 flames at ϕ=1.0 as a function of $X_{O_2,ox}$. The solid line is a linear least-squares regression curve fit to the data, and the dotted line is the calculated value.

From the curve fits to the experimental data in Figure 4, we observe that the maximum value of the burning velocity occurs for slightly fuel-lean flames. For example, with $X_{O_2,ox}$ = 0.32, a peak value of the burning velocity (36.5±3.0) cm/s occurs at ϕ=0.83, and with $X_{O_2,ox}$ = 0.365, the peak value of the burning velocity (43.6±2.7) cm/s occurs at ϕ=0.90. Unlike hydrocarbon flames, which have peak burning velocities at slightly fuel-rich conditions; e.g. ethylene-air flame have their peak S_L at ϕ=1.13, the peak flame speed for TDCE occurs for the leaner flames, and this effect is more pronounced for flames at lower $X_{O_2,ox}$.

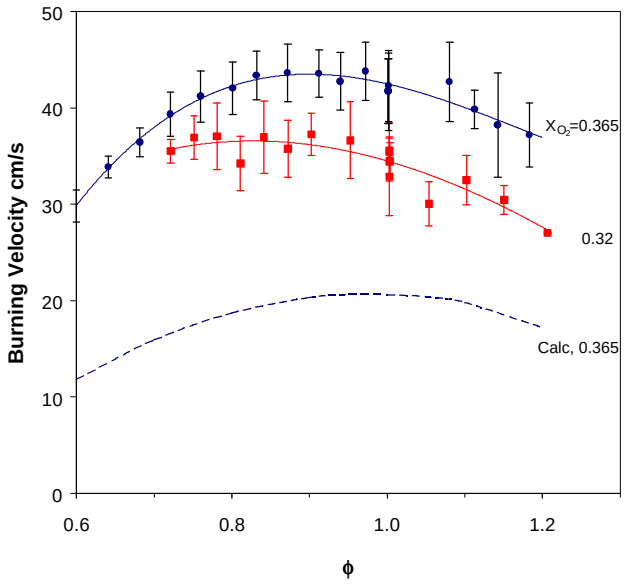

Figure 4 – Burning velocity of pure TDCE flames at $X_{O_2,ox}$ = 0.32 and 0.365 as a function of ϕ. Solid lines are curve fits to the experimental data.

In Figure 1, the numerically calculated burning velocity for ϕ=1.0 (dotted line) is in good agreement with the experimental data for pure methane-air flames. As the fraction of TDCE in the fuel mixture increases, however, the discrepancy between the measured and predicted flame speed increases. At a TDCE mole fraction in the fuel stream of about 0.75, the numerical calculation yields a flame speed about a factor of two lower than the experiment. (Note that we had difficulty obtaining converged solutions for higher fractions of TDCE in the fuel stream.) Similarly, Figure 3 shows that the calculated burning velocity for stoichiometric flames is about a factor of two lower for all values of $X_{O_2,ox}$ tested, while Figure 4 also shows an underprediction for S_L for $X_{O_2,ox}$ = 0.365, over the range 0.65 >= ϕ <= 1.2.

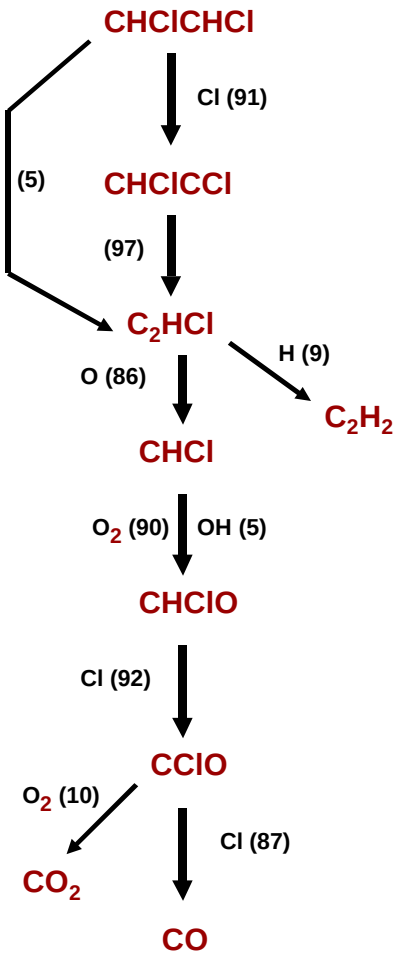

Figure 5 – Reaction pathway for decomposition of TDCE.

We have studied the numerical results in an effort to understand the reasons for the under-prediction of the burning velocity. Figure 5 shows the calculated decomposition pathway for pure TDCE at ϕ=1.0 and $X_{O_2,ox}$ = 0.365. Consumption of TDCE proceeds mostly through the reaction with chlorine atom leading to CHClCCl radical, which then loses an H atom to form C_2HCl. Chloroacetylene is consumed primarily through reaction with O to form chloromethylene (CHCl), while some reaction with H atom forms acetylene. Approximately 90% of chloromethylene is consumed by reaction with oxygen molecule with the formation of formyl chloride (CHClO). CHClO reacts mostly with chlorine atom leading to carbonyl chloride (CClO). At this stage, the reaction of CClO with Cl to form CO completes the main reaction pathway for consumption of the chlorocarbon species. Approximately 10% of CClO is consumed in reaction with O_2 with direct formation of CO_2. The reaction pathway for TDCE consumption is similar to that for ethylene consumption, with some of the important H-atom reactions replaced by those of Cl. Because of this, the separation of the fuel decomposition chemistry (here,

dominated by Cl radicals) from the CO consumption regions (dominated by the H, O, OH radical pool) is even more distinct than in hydrocarbon flames.

We have also calculated the first-order sensitivity coefficient of the burning velocity with respect to the specific reaction rate constant for each reaction. Table 1 presents all values of the sensitivity which are greater than 1% of the maximum value. As in hydrocarbon flames, the H + O_2 branching reaction and the CO + OH reaction have the highest sensitivities. The chlorine reactions with the highest sensitivities are:

$C_2HCl + O = CHCl + CO$
$Cl_2 + H = HCl + Cl$
$Cl + Cl + M = Cl_2 + M$
$CClO + O_2 = CO_2 + ClO$
$CClO + Cl = CO + Cl_2$
$CHCl + O_2 = CHClO + O$
$HCl + O = OH + Cl$
$CHCl + OH = CHClO$.

We attempted to improve the agreement between experiment and model. We varied the rate constants by a factor of 2 to 10 for reactions with a large sensitivity coefficient (taking into consideration the reported uncertainty in the rate constant). We also varied the enthalpy of formation to account for uncertainties in the data for some important species. We included additional chain branching steps involving vibrationally excited molecules; e.g., H + Cl_2 = HCl* + Cl, HCl* + Cl_2 = HCl + Cl_2*, Cl_2* = 2Cl, HCl* + M = HCl + M, as suggested by Leylegian et al. (1999). Finally, we included some additional reactions and experimented with transport properties. Unfortunately, none of these tests provided significant improvements in the model predictions. There may be additional important reaction pathways which are not presently included in the mechanism. These may include reactions of excited state C_2 species alluded to by Qun and Senkan (1994).

The results shown in the figures above indicate that while the mechanism works reasonably well at predicting the behavior of the system at low TDCE loading, it becomes less accurate for pure TDCE. Recalling that the sub-mechanisms upon which the present full mechanism was developed were validated using data from experiments with other chlorohydrocarbons mixed with larger amounts of methane, it is reasonable that the mechanisms work best in this regime. Clearly, additional work is necessary to extend the mechanism to conditions of pure TDCE combustion.

Table 1 – First-order Sensitivity Coefficient of the Burning Velocity with respect to the Specific Reaction Rate Constant.

Reaction	**Sensitivity**
$O+OH = O_2+H$	1.29E-01
$CO+OH = CO_2+H$	1.10E-01
$C_2HCl+O = CHCl+CO$	8.17E-02
$Cl_2+H = HCl+Cl$	-6.66E-02
$Cl+Cl+M = Cl_2+M$	6.51E-02
$CClO+O_2 = CO_2+ClO$	3.57E-02
$CClO+Cl = CO+Cl_2$	-3.16E-02
$CHCl+O_2 = CHClO+O$	2.77E-02
$HCl+O = OH+Cl$	-1.53E-02
$CHCl+OH = CHClO+H$	-1.14E-02
$Cl_2+O = Cl+ClO$	8.90E-03
$C_2Cl_2+O = CO+CCl_2$	-8.30E-03
$HCl+OH = Cl+H_2O$	-7.70E-03
$C_2H_2+O_2 = HCCO+OH$	7.48E-03
$CHCl+O_2 = CO+HOCl$	-7.47E-03
$CHCl+O = CO+HCl$	-7.16E-03
$HCO+M = CO+H+M$	6.67E-03
$Cl+HCO = CO+HCl$	-6.25E-03
$C_2HCl+H = C_2H_2+Cl$	-6.00E-03
$CHClCHCl = CHCHCl+Cl$	4.24E-03
$CHCl_2CHCl_2 = CHClCHCl_2+Cl$	-4.19E-03
$CH_2+O_2 = CH_2O+O$	3.69E-03
$C_2Cl_2+O_2 = CClO+CClO$	3.06E-03
$C_2Cl_2+H = C_2HCl+Cl$	-3.03E-03
$CHClCHCl = C_2HCl+HCl$	-2.98E-03
$O_2+CO = O+CO_2$	2.76E-03
$C_2H_2+O = HCCO+H$	-2.67E-03
$CH+CO(+M) = HCCO(+M)$	2.58E-03
$HOCl = Cl+OH$	2.50E-03
$HCCO+O = H+_2CO$	-2.18E-03
$CHClO+Cl = CClO+HCl$	-2.17E-03
$CHClCCl+O_2 = CClO+CHClO$	2.16E-03
$CH_3+Cl = CH_2+HCl$	-2.06E-03
$CHCHCl+O_2 = HCO+CHClO$	1.79E-03
$CHClCHCl_2+Cl = C_2HCl_3+HCl$	-1.78E-03
$CHClCHCl+Cl = CHClCCl+HCl$	1.58E-03
$CHCl_2+O = CHClO+Cl$	-1.55E-03
$HCl+H = H_2+Cl$	1.53E-03
$C_2HCl+OH = CH_2CO+Cl$	1.42E-03
$CHClO = HCO+Cl$	1.36E-03
$CHClCHCl+O = HCO+CHCl_2$	-1.35E-03

An understanding of the kinetic mechanism for pure TDCE combustion is desirable. Such a mechanism would give us more confidence in the functional form of the extrapolations of the burning velocity measurements to the desired conditions of pure TDCE at $X_{O_2,ox}$ = 0.21. Further, it is likely that in incinerators, mixing limitations will create regions in which the ratio of TDCE to methane is very high, so that the reaction kinetics will be dominated by those of TDCE rather than methane. Present mechanisms, developed for lower CHC loadings may not accurately predict reactions sequences occurring under actual full-scale conditions.

CONCLUSIONS

We present the first burning velocity measurements for 1,2-trans-dicholorethylene alone and with methane, over a range of ϕ and $X_{O_2,ox}$. Through extrapolations, we have estimated the burning velocity of pure TDCE with air to be (10.7±1.2) cm/s. We have performed numerical calculations of the burning velocity and flame structure of these flames, and compared experiments and calculations. The predicted burning velocities are found to be in good agreement for low TDCE loadings in methane; however, for pure TDCE, the calculated S_L is about a factor of two lower than the experimental results, indicating that some important reactions are likely missing in the kinetic model. Further research on this system appears to be warranted.

References

Andrews, G. E. and Bradley, D., 1972, "Determination of burning velocities: a critical review," Combustion and Flame, Vol. 18, pp. 133-153.

Babushok, V., Tsang, W., and Noto, T, 2000, "Propargyl type radicals as precursors for polychlorinated aromatic hydrocarbons during incineration," Proceedings of the Combustion Institute, Vol. 28, The Combustion Institute, Pittsburgh, PA, pp. (to appear).

Castaldi, M. J. and Senkan, S. M., 1996, "Chemical structures of fuel-rich flames of trans-$C_2H_2Cl_2/CH_4/Ar/O_2$ mixtures," Combustion and Flame, Vol. 104, pp. 41-50.

Ho, W. P., Booty, M. R., Magee, R. S., and Bozzelli, J. W., 1995, "Analysis and optimization of chlorocarbon incineration through use of a detailed reaction mechanism," Industrial & Engineering Chemistry Research, Vol. 34, pp. 4185-4192.

Kee, R. J., Dixon-Lewis, G., Warnatz, J., Coltrin, R. E., and Miller, J. A., 1986, "A Fortran Computer Package for the Evaluation of Gas-Phase, Multicomponent Transport Properties," SAND86-8246.

Kee, R. J., Grcar, J. F., Smooke, M. D., and Miller, J. A., 1991, "A Fortran Computer Program for Modeling Steady Laminar One-dimensional Premixed Flames," SAND85-8240.

Kee, R. J., Rupley, F. M., and Miller, J. A., 1989, "CHEMKIN-II: A Fortran Chemical Kinetics Package for the Analysis of Gas Phase Chemical Kinetics," SAND89-8009B.

Leylegian, J. C., Law, C. K., and Wang, H., 1998, "Laminar flame speeds and oxidation kinetics of tetrachloromethane," Proceedings of the Combustion Institute, Vol. 27, The Combustion Institute, Pittsburgh, PA, pp. 529-536.

Leylegian, J. C., Law, C. K., and Wang, H., 1999, "On the branched-chain mechanism of hydrogen-chlorine reactions: laminar flame speed experiments and kinetic modeling of $H_2/Cl_2/N_2$ mixtures," Proceedings of the Fall Technical Meeting of the Combustion Institute, The Combustion Instutute, Pittsburgh PA, pp. 367-370.

Leylegian, J. C., Zhu, D. L., Law, C. K., and Wang, H., 1998, "Experiments and numerical simulation on the laminar flame speeds of dichloromethane and trichloromethane," Combustion and Flame, Vol. 114, pp. 285-293.

Linteris, G. T., Rumminger, M. D., and Babushok, V. I., 2000, "Premixed carbon monoxide-nitrous oxide-hydrogen flames: measured and calculated burning velocities with and without $Fe(CO)_5$," Combustion and Flame, Vol. 122, pp. 58-75.

Linteris, G. T. and Truett, L., 1996, "Inhibition of premixed methane-air flames by fluoromethanes," Combustion and Flame, Vol. 105, pp. 15-27.

Mache, H. and Hebra, A., 1941, Sitzungsber. Österreich. Akad. Wiss., Abt. IIa, 150, pp. 157.

Mallard, W. B., Westley, F., Herron, J. T., Hampson, R. F., and Frizzell, D. H., 1994, *NIST Chemical Kinetics Database: Version 6.0*, National Institute of Standards and Technology, Gaithersburg, MD.

Mertens, J. A., 1991, "Dicholorethylene," in Encyclopedia of Chemical Technology, Kirk, R. E., Ed., Wiley, New York, pp. 36-40 .

Noto, T., Babushok, V., Hamins, A., and Tsang, W., 1998, "Inhibition effectiveness of halogenated compounds," Combustion and Flame, Vol. 112, pp. 147-160.

Qun, M. and Senkan, S. M., 1994, "Chemical kinetic modeling

of fuel-rich flames of $CH_2Cl_2/CH_4/O_2/Ar$," Combustion Science and Technology, Vol. 101, pp. 103-134.

Thomson, M. J., Higgins, B. S., Lucas, D., Koshland, C. P., and Sawyer, R. F., 1994, "Phosgene formation from 1,1,1-trichloroethane oxidation," Combustion and Flame, Vol. 98, pp. 350-360.

Thomson, M. J., Lucas, D., Koshland, C. P., Sawyer, R. F., Wu, Y. P., and Bozzelli, J. W., 1994, "An experimental and numerical study of the high-temperature oxidation of 1,1,1-$C_2H_3Cl_3$," Combustion and Flame, Vol. 98, pp. 155-169.

UTHSCA, 1996, ImageTool, V2.00. Image Tool is a free Windows95-based program developed at the University of Texas Health Science Center at San Antonio, Texas and available from the Internet by anonymous FTP from ftp://maxrad6.uthscsa.edu or http://ddsdx.uthscsa.edu

Van Wonterghem, J. and Van Tiggelen, A., 1954, "L'epaisseur et la vitesse de propagation du front de flamme," Bulletin des Societes Chimiques Belges, Vol. 63, pp. 235-260.

Wang, H., Hahn, T. O., Sung, C. J., and Law, C. K., 1996, "Detailed oxidation kinetics and flame inhibition effects of chloromethane," Combustion and Flame, Vol. 105, pp. 291-307.

Wang, H., Sung, C. J., and Law, C. K., 1997, "On mild and vigorous oxidation of mixtures of chlorinated hydrocarbons in droplet burning," Combustion and Flame, Vol. 110, pp. 222-238.

Zalosh, R. G., 1995, "Explosion protection," in SFPE Handbook of Fire Protection Engineering, Society of Fire Protection Engineers, Boston, pp. 3-312 - 3-329.